Australian Government
Department of Defence
Defence Science and
Technology Organisation

Phase II Experimental Testing of a Generic Submarine Model in the DSTO Low Speed Wind Tunnel

Howard Quick and Bruce Woodyatt

Aerospace Division
Defence Science and Technology Organisation

DSTO-TN-1274

ABSTRACT

DSTO has completed the second phase of an experimental test program on a sub-scale model of a generic submarine in its low-speed wind tunnel. These tests were used to gather gross steady-state aerodynamic force and moment data for the model in various configurations, where different appendages including a hull-casing, a fin, and control surfaces were incrementally added to the bare-hull form. The effectiveness of the control surfaces to induce pitch and yaw motions was also investigated.

Published by

Aerospace Division
DSTO Defence Science and Technology Organisation
506 Lorimer St
Fishermans Bend, Victoria 3207 Australia

Telephone: 1300 333 362
Fax: (03) 9626 7999

AR-015-873
March 2014

APPROVED FOR PUBLIC RELEASE

Phase II Experimental Testing of a Generic Submarine Model in the DSTO Low Speed Wind Tunnel

Executive Summary

Defence Science and Technology Organisation (DSTO) researchers are undertaking a comprehensive study of the flow characteristics around modern submarine geometries to enhance their knowledge and understanding of these complex flow phenomena. Conducted under the auspices of the DSTO Corporate Enabling Research Programme (CERP) - Future Undersea Warfare, the research involves the use of high-fidelity computational fluid dynamic (CFD) methods, as well as extensive experimental hydrodynamic and aerodynamic testing of a generic shape that is representative of a modern diesel-electric powered submarine.

A sub-scale model of a generic submarine has been tested in the DSTO low-speed wind. The model, as tested, was a 1.35 m long aluminium representation of a submarine, and included a number of detachable appendages, namely a hull-casing, a fin, and four moveable control surfaces. These tests, designated phase II, follow on from previous wind tunnel testing of the same model in bare-hull configuration, now focus specifically on the measurement of gross steady-state forces and moments as various appendages were fitted to the model. The aims of the experiment were to quantify the incremental effects of each appendage, and to assess the effectiveness of the control surfaces at inducing pitch and yaw motions.

This report describes the experimental equipment used during the tests, and the test methodology. Selected results from the experiments are also presented and briefly discussed. Overall, the force and moment data were generally consistent and repeatable, exhibiting expected trends. The results from these tests will add to a database of information already compiled for this generic submarine shape, and provide a source of comparative data for computational testing of the same configuration. The wind tunnel experiments will also be used to inform future experimental studies involving the testing and analysis of modern submarine shapes in the DSTO low-speed wind tunnel.

This page is intentionally blank

Contents

List of Figures

List of Tables

This page is intentionally blank

Notation

C_D	Drag force coefficient $\left(\frac{D}{qS}\right)$
$[C_K, C_M, C_N]$	Roll, pitch and yaw moment coefficients $\left[\left(\frac{K}{qSl}\right),\left(\frac{M}{qSl}\right),\left(\frac{N}{qSl}\right)\right]$
C_L	Lift force coefficient $\left(\frac{L}{qS}\right)$
$[C_X, C_Y, C_Z]$	Surge, Sway and Heave force coefficients $\left[\left(\frac{X}{qS}\right),\left(\frac{Y}{qS}\right),\left(\frac{Z}{qS}\right)\right]$
CG	Centre of gravity
d	Body diameter (0.185 m)
D	Drag force (N)
$[K, M, N]$	Moment about the x-axis, y-axis, z-axis (Nm)
l	Model reference length (1.35 m)
L	Lift force (N)
MRP	Moment Reference Point
q	Dynamic pressure $\left(\frac{1}{2}\rho U^2\right)$ (Pa)
Re_l	Reynolds number $\left(\frac{\rho U l}{\mu}\right)$
S	Model reference area (1.8225 m^2, where $S = l^2$)
$[u, v, w]$	Velocity components along x-axis, y-axis, z-axis
U	Free-stream wind tunnel air velocity (m/s)
$[X, Y, Z]$	Surge, Sway, Heave force (N)
α	Angle-of-attack (^{o})
β	Angle-of-drift (^{o})
ρ	Density (kg/m^3)
μ	Viscosity (kg/m.s)
σ	Standard deviation

This page is intentionally blank

1. Introduction

This report describes the testing of a sub-scale generic submarine model in the DSTO low-speed wind tunnel (LSWT) during March 2012, and follows earlier experimental work conducted in mid-2010, using the same model in bare-hull configuration [1]. The aim of this latest series of tests, hereafter referred to as phase II, was to gather gross steady-state aerodynamic force and moment data for the model in various configurations, that is, with different appendages fitted. The appendages tested included a hull-casing, a fin, and four moveable control surfaces, where each component was added separately to the bare-hull form. This build-up approach enabled the aerodynamic influence of each component to be quantified. The data from the wind tunnel tests together with results from computational fluid dynamic (CFD) studies will be used by researchers to enhance their knowledge and understanding of the complex flows around modern submarine shapes, particularly large diesel-electric powered vessels.

This report details the experimental equipment used during the phase II wind tunnel tests, including descriptions of the model, the test facility, and the instrumentation used to gather the data. A section on experimental method defines the axes systems and reference coordinates used, the data reduction methods, the corrections applied to the results, the test conditions, and the test schedule. A sample of the data that were gathered is also presented, and these results are briefly discussed.

2. Experimental Equipment

2.1 Generic Submarine Model

The sub-scale generic submarine model was designed and manufactured to be suitable for use in both a wind tunnel, and with minor modifications, a water tunnel. Machined from aluminium, the bare-hull form comprises a uniform cylindrical centre-body with an elliptical nose, and a streamlined after-body section. A number of appendages were also manufactured (i.e. hull-casing, a fin, and four moveable aft control surfaces arranged in an X configuration), and when fully appended, the model approximates the geometric form of a modern diesel-electric powered submarine. Further information regarding the hydrodynamic design criteria applied to the submarine model is presented in Reference [2].

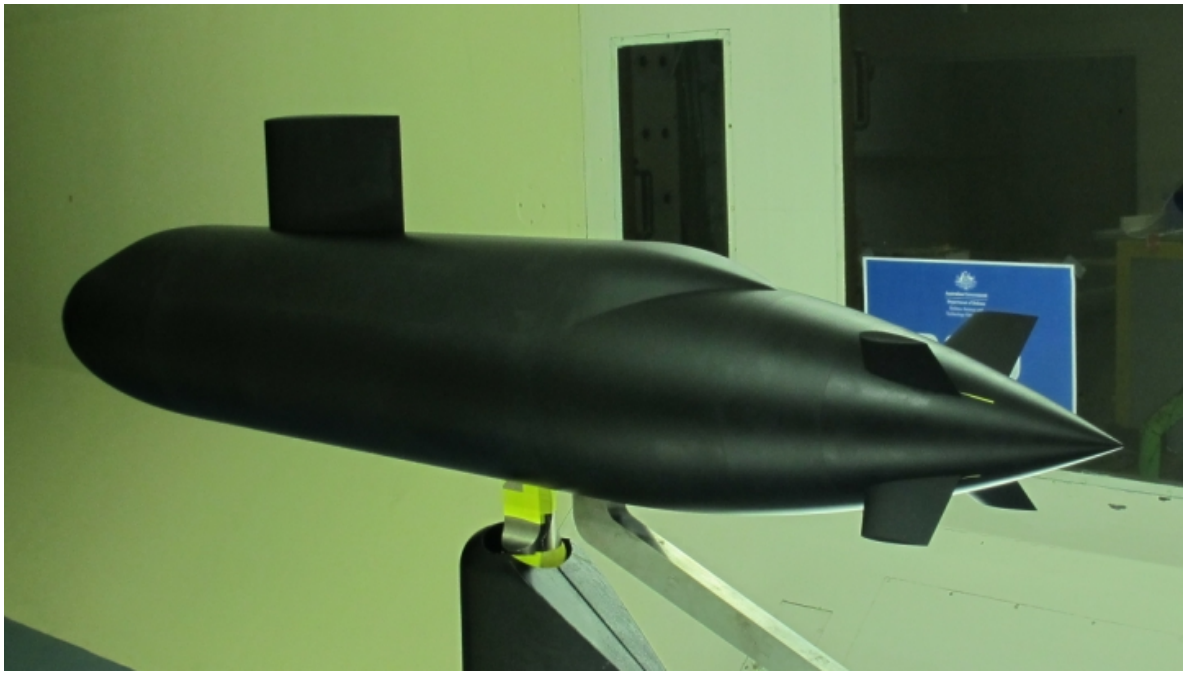

Figure 1 - Generic submarine model mounted in the DSTO low-speed wind tunnel in its fully-appended configuration.

Figure 1 shows the model mounted in the LSWT on a single, vertical support pylon, where pitch attitude is controlled via a pitch–arm. The vertical support pylon is shrouded by a detachable aerodynamic fairing that is in-turn mounted on a rotating turn-table. This apparatus allows the model assembly to be yawed (i.e. drift angle applied) relative to the free-stream flow. Importantly, the aerodynamic fairing remains aligned with the free-stream flow at all times. The model was also fitted with an internal six-component strain gauge balance, enabling gross steady-state aerodynamic force and moment data to be gathered. A cut-away schematic view of the model in its bare-hull form is shown in Figure 2, and illustrates the location of the pivot attachment point on the pitch-arm, the internal strain gauge balance, and the inclinometer in the forward section of the hull used to measure pitch-angle.

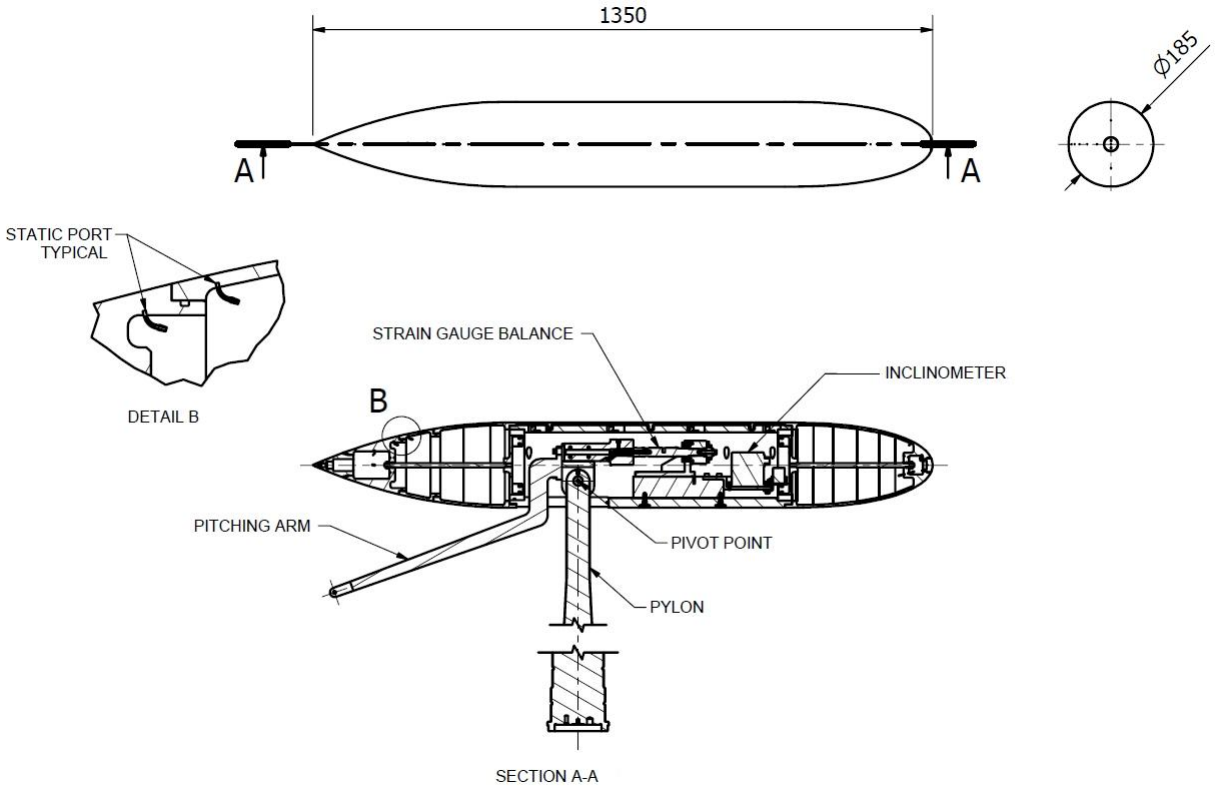

Figure 2 - Schematic cut-away drawing of the generic submarine model in its bare-hull form.

2.2 DSTO Low-Speed Wind Tunnel

The experimental tests were conducted in the DSTO LSWT located at Fishermans Bend in Melbourne. This facility is a conventional subsonic, closed-circuit wind tunnel that is capable of airspeeds up to 100 m/s. The test-section has an irregular octagonal cross-section measuring 2.74 m (wide) by 2.13 m (high). The maximum unit Reynolds number per metre is approximately 6 x 10^6 based on the maximum airspeed achievable during a test. Further technical specifications for the wind tunnel and its data acquisition system are provided in Table A1 and Table A2 respectively of Appendix A.

2.2.1 Blockage Ratio

The blockage ratio for the fully-appended model at the maximum angle-of-drift tested (i.e. $\beta = 30^o$) was estimated to be 3.5%. This value is based a model frontal area component (i.e. 1.9%) and a 1.6% contribution from the vertical pylon fairing. Importantly, this value of blockage ratio is substantially lower than the maximum ratio of 7.5% which is widely regarded as acceptable value in subsonic wind tunnel testing [3].

2.3 Strain Gauge Balance

A six-component strain gauge balance was fitted inside the model, and used to measure gross steady-state aerodynamic forces and moments as the model was pitched and yawed through a range of discrete angles. Figure 3 shows the strain gauge balance used throughout the tests, whilst details of its calibrated load range are provided in Table A3 of Appendix A

Figure 3 - Strain gauge balance DSTO-BAL-04.

The strain gauge balance used in these tests was the same device used during the previous (i.e. phase I) low-speed wind tunnel tests [1]. However, it should be noted that in the intervening period between the two test campaigns, the balance was returned to the original equipment manufacturer for inspection and full calibration. To ensure that the performance of device was consistent, a number of test points from the previous experiments were repeated in these tests. Importantly there were no discernable changes in the quality of the results between the two test campaigns. These comparative results are discussed later in this report.

3. Experimental Method

The experimental method employed during the phase II tests is described below, and includes details of the axes system and reference coordinates, and data reduction. The test conditions are also reported, along with a brief description of the test schedule. Issues pertinent to data processing and data accuracy are also canvassed.

3.1 Axes System

The model was tested at various attitudes, as defined by combinations of angle-of-attack (α) and angle-of-drift (β). An inclinometer, a Jewel Instruments LCF-3000 unit, was fitted inside the model to measure α, whilst β was measured by the turntable encoder. Gross steady-state aerodynamic force and moment data were gathered in a body-axes system, and reduced to their non-dimensional coefficient form. Figure 4 defines the body-axes system used during these tests.

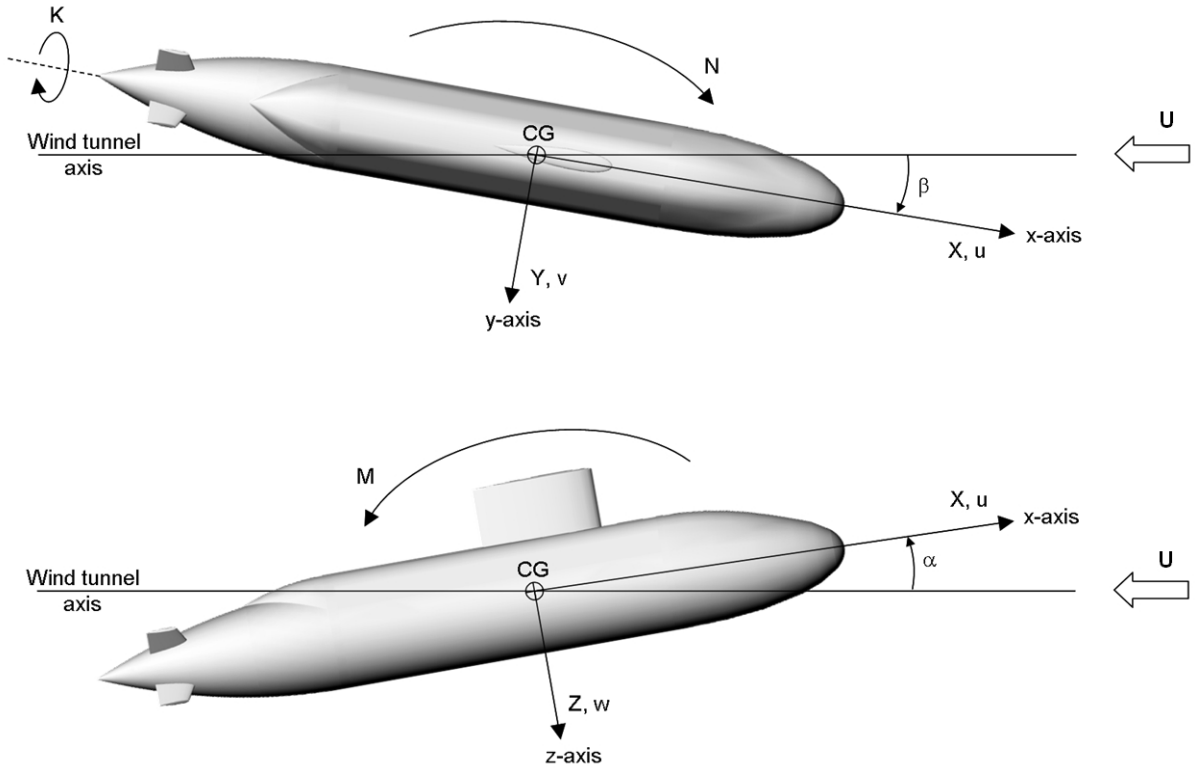

Figure 4 – Axes system.

3.2 Reference Coordinates

The aerodynamic force and moment data were measured relative to a moment reference point (MRP). The moment reference point was defined as the mid-length position on the centre-line of the model. Figure 5 presents the moment reference point and also the location of the strain gauge balance. The reference centre of the strain gauge balance was located 77.64 mm axially forward, and 28.0 mm vertically above the defined moment reference point. These coordinates were consistent with previous wind tunnel testing of the model [1].

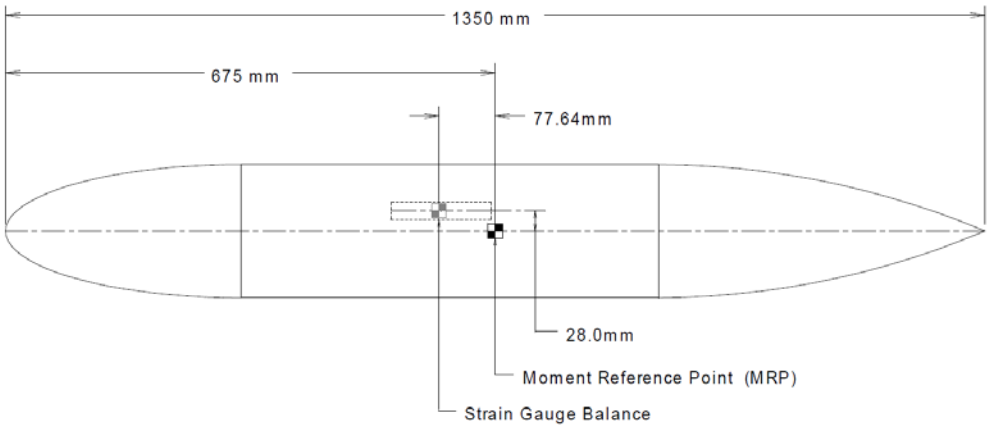

Figure 5 - Model reference coordinates.

3.3 Data Reduction

The force and moment data were reduced to their non-dimensional coefficient form using the reference parameters defined in Table 1.

Table 1 - Reference parameters for the generic submarine model.

Reference Parameter	Value	Units
Length (l)	1.35	m
Area ($S = l^2$)	1.8225	m^2

Where, the aerodynamic forces and moments expressed as coefficients take the form;

$$C_X = \left(\frac{X}{qS}\right), \qquad C_Y = \left(\frac{Y}{qS}\right), \qquad C_Z = \left(\frac{Z}{qS}\right),$$

$$C_K = \left(\frac{K}{qSl}\right), \qquad C_M = \left(\frac{M}{qSl}\right), \qquad C_N = \left(\frac{N}{qSl}\right) \qquad \text{... (1)}$$

In Equation (1), C_X, C_Y and C_Z represent the force coefficients in the x, y and z body-axes respectively; C_K, C_M and C_N are the corresponding moment coefficients about these axes (refer Figure 4); q is the dynamic pressure, and S and l are reference parameters as defined

in Table 1. Similarly, the lift and drag coefficients C_L and C_D respectively are defined in Equation (2) as:

$$C_L = \left(\frac{L}{qS} \right), \qquad C_D = \left(\frac{D}{qS} \right) \qquad \text{... (2)}$$

3.4 Flow Offsets

Flow offsets, or flow angularities, represent the change in flow angle due to the presence of the model and its support equipment in the flow-field. Whilst flow offsets were estimated in the phase I tests [1], they were not estimated in these tests since the model arrangement (i.e. pylon mount) and free-stream velocity (i.e. 60 m/s) were the same in both test campaigns. Furthermore, since the focus of this phase of testing was the estimation of incremental effects, the data gathered were not corrected for flow offsets. For completeness, table 2 shows the flow offsets estimated in phase I.

Table 2 - Flow offset angles.

Flow Direction	Value
Cross-flow	0.24°
Up-flow	1.8°

3.5 Test Conditions

3.5.1 Reynolds Number

The wind tunnel tests were conducted at a nominal airspeed of 60 m/s representing a Reynolds number Re_l of 5.2 x 10^6, based on body length (l). For comparison purposes, a typical full-scale equivalent diesel-electric submarine operating in seawater at 20 knots would have a corresponding Reynolds number of approximately 6 x 10^8.

3.5.2 Boundary Layer Transition

To better approximate the behaviour of the boundary layer over a typical, full-scale, submarine, a transition strip was attached to the model. An empirical method, described in reference [4], was used to determine the appropriate carborundum grit size (i.e. size 80, or an average particle diameter of 0.21 mm) for use in this test program. As Figure 6 shows, a 3 mm wide transition strip was attached circumferentially around the body of the model, approximately 67.5 mm downstream from the nose, or at 5% of the reference body length (l). The size and location of this transition strip was consistent with phase I testing of the model [1]. No transition trips were used on the hull-casing, fin or aft control surfaces.

Figure 6 - Boundary layer transition strip attached circumferentially at 5% of the model length (l).

3.6 Test Schedule

The primary aim of the phase II tests was to gather gross steady-state aerodynamic force and moment data for the model in various configurations (i.e. with different appendages fitted). This build-up approach was used to compile an incremental database, that is, information that characterises the (discrete) influences of the hull-casing, fin, and control surfaces on the full-configuration. In addition, the tests also provided an opportunity to investigate the effectiveness of the control surfaces in pitch and yaw. A brief description of the main elements of the phase II test program are reported here, and for completeness a copy of the test schedule is included in Table B1 of Appendix B.

3.6.1 Reference Runs

To quantitatively assess the consistency and repeatability of the experimental method, and to confirm the performance of the strain gauge balance, DSTO-BAL-04, across the two test campaigns, the model in its bare-hull configuration with the transition strip-on[1], was pitched and yawed through a range of α and β at an airspeed of 60 m/s. The model configuration and test conditions were the same as those reported in [1]. The results for the *Reference Runs* from both test campaigns are compared in Appendix C.

3.6.2 Bare-Hull – Boundary Layer Transition Strip-Off

The model in the bare-hull configuration was tested at free-stream velocities of 30 m/s, 40 m/s, and 60 m/s with boundary layer transition strip-off, with data gathered at various combinations of α between $\pm 15^{o}$ and β between $\pm 30^{o}$. The same series of tests were also conducted in phase I.

[1] Reference Runs with transition strip-on refers to the attachment of a transition strip around the circumference of the model at 5% of its body length.

3.6.3 Bare-Hull – Boundary Layer Transition Strip-On

The model in its bare-hull configuration was also tested with boundary layer transition strip-on at free-stream velocities of 30 m/s, 40 m/s, and 60 m/s. During these tests a transition strip was attached around the circumference of the model at 5% of its body length. At each velocity, the model was pitched and yawed at various combinations of α between $\pm 15^{o}$ and β between $\pm 30^{o}$. The same series of tests were also conducted in phase I and results from both phases are compared.

3.6.4 Configuration Build-up Test

In order to quantify the change in forces and moments due to the addition of each appendage (i.e. hull-casing, fin, and the control surfaces), a configuration build-up approach was used, with the bare-hull configuration used as the baseline test article. This involved pitching the model at zero β, and yawing the model at zero α in its bare-hull configuration with the transition strip-on at a free-stream velocity of 60 m/s. The control surfaces were then fitted to the model in their neutral position and the test repeated. The hull-casing was then added to the bare-hull and control surfaces, and the same test sequence was repeated again. Finally the fin was added to represent the full-configuration, and the test sequence repeated.

3.6.5 Full-Configuration with Control Surfaces Deflected

Data were gathered for the model in the full-configuration with the transition strip-on, where different combinations of control surfaces were deflected at ±3°. These tests were used to assess the effectiveness of the control surfaces to induce pitch and yaw responses. These tests were also conducted over a set range of α and β angles at a free-stream velocity of 60 m/s.

4. Results

Selected results from the wind tunnel tests are briefly discussed below, and presented graphically in Appendix C to Appendix F. Whilst these results represent only a sub-set of all of the data gathered, the significant aspects of the test program are covered. Where applicable, data from phase I are also presented. The discussion of the results is intentionally brief and of a qualitative nature, and a more thorough analysis and assessment of the results will be the subject of future reports.

4.1 Reference Runs

Appendix C shows the force and moment data gathered during the *Reference Runs*. Plotted in their body-axes coefficient form, the results represent the model in its bare-hull configuration with the transition strip-on. Since the model was also tested in this

configuration and at the same conditions in phase I, these results are also reported. Error bars are used to illustrate the 2σ confidence (uncertainty) limits on the data.

4.1.1 Effect of Pitch Angle on Forces and Moments

The results in Figure C 1 show that the data are consistent and repeatable, and within the bounds of acceptable experimental error (i.e. the results for each coefficient are generally within a 2σ-band about a mean). Furthermore, there are no discernable differences between the data gathered in each of the test campaigns. Each of the coefficients is expressed as a function of α over the range ±15° at zero β. Ideally, given the symmetry of the bare-hull configuration, the results for the surge-force coefficient in the body-axis (C_X) should be approximately symmetric about zero α. However, the results display a positive, non-linear gradient over the majority of the range of conditions tested. This asymmetry in the data is most likely due to the adverse influence of the vertical support pylon and fairing on the flow-field. In contrast, the heave-force coefficient in the body-axis (C_Z) is relatively symmetric over the range of conditions tested, albeit with a small non-zero value of C_Z at zero α. These data exhibit a predictable change in gradient with α, and are consistent with increased body lift with increasing α. The pitching moment coefficient (C_M) has a positive gradient, that is, C_M increases with increasing α. These results also show a small offset in C_M at zero-incidence, and are indicative of an asymmetry in the flow due to the model mount arrangement (i.e. there is a tendency for nose-up pitch at this attitude).

The C_Y, C_K and C_N coefficients show relatively minor changes for varying α at zero β. The magnitudes of these variations are small and fall within the bounds of acceptable experimental error. The sway-force coefficient in the body-axis (C_Y) is approximately constant in pitch over the range of conditions tested (i.e. pitching the model either nose-up or nose-down does not significantly influence C_Y). The rolling moment coefficient (C_K) is also relatively insensitive to changes in α, albeit the data does show a small negative gradient over the range of conditions tested. Similarly, the results for the yawing moment coefficient (C_N) highlight an asymmetry in the flow about zero-incidence.

4.1.2 Effect of Drift Angle on Bare-Hull Forces & Moments

The effect of drift angle on bare-hull forces and moments are shown in Figure C 2 for phase II testing only, as comparable data from earlier testing was not available. These results show that overall the data are consistent and repeatable, and fall within the 2σ bands of experimental error. Each of the coefficients is expressed as a function of β over the range ±30° at zero α.

The sway-force coefficient (C_Y) is asymmetric about zero β, exhibiting a positive, non-linear gradient over the conditions tested. As expected, C_N exhibits similar trends. Given the symmetry of the bare-hull configuration model, C_K should be insensitive to changes in β; however, the data does show a small change in gradient over the range of conditions tested. Overall, the gradient is well within the bounds of experimental error.

There are some noteworthy trends in the surge and heave coefficients, with considerable changes in magnitudes of these coefficients with β. For example, the coefficients C_M and C_Z are relatively constant for angles of drift of $-10^o < \beta < +10^o$, but as drift angle increases their magnitudes change significantly; furthermore, the data are approximately symmetric about zero β. These trends may again be explained by the adverse influence of the support pylon and fairing on the flow-field, and the effect of cross-flow as the model is yawed at moderate-to-high angles of β. The model support structure is responsible for the formation of a wake downstream of the fairing, and this influences the flow-field over the aft-end of the model. This wake region interacts with cross-flow vortices over the body and serves to decrease C_Z, or increase the lift over the aft-body, and manifests in a nose-down pitching moment.

4.2 Configuration Build-up Tests

The purpose of this series of tests was to quantitatively assess the incremental effects of various appendages fitted to the bare-hull configuration. Using a configuration build-up approach, a hull-casing, control surfaces (i.e. fixed in their neutral positions), and a fin were added to the bare-hull, and the resultant forces and moments were measured. The incremental coefficients were then determined by subtracting the bare-hull data from the built-up configuration data at the same test condition. Incremental force and moment coefficients are presented to better illustrate the relative effect of each of the appendages.

4.2.1 Effect of Pitch Angle

Figure D 1 shows the incremental forces and moments as the model was pitched through a range of α at zero β. As expected, pitching the model has most influence on the C_X, C_M, and C_Z, coefficients with the control surfaces particularly influencing the heave-force and pitch characteristics. A noteworthy observation is the lack of asymmetry in both C_M and C_Z about zero α, that is, the change in the magnitude of both coefficients is less when the model is pitched nose-up compared to pitching the model nose-down. These results again illustrate the adverse influence of the model support structure on the flow-field, particularly as the aft-body of the model is affected by this wake region at positive incidences. For all of the configurations tested, C_X was most negative (i.e. drag was highest) when the model was in its fully-appended state.

In Figure D 1 it is more difficult to discern the impact of the various appendages on the C_K, C_Y, and C_N coefficients. These coefficients are relatively invariant with changes in pitch angle.

4.2.2 Effect of Drift Angle

Figure D 2 shows the incremental forces and moments for the configuration build-up as the model was yawed through a range of β at zero α. Unlike the predictable nature of the results for the model in pitch, yawing the model with the fin attached affected all six coefficients, indicating a cross-coupling effect with drift angle. The fin acts as a low aspect ratio lifting surface on the model, and generates significant flow-field effects at moderate-

to-high drift angles. The influence of the fin is clearly evident in the C_K, C_Y, and C_N coefficients. In each case, the magnitude of these coefficients increases linearly with β. The fin has a marked effect on the C_X, C_Z, and C_M coefficients, with non-linear trends indicated in the results. Other components, such as the hull-casing or control surfaces, generally had significant effects, and were relatively invariant at small-to-moderate angles of β. The pronounced influence of the fin on all coefficients is most likely due to the complex interaction of the vortex structures from the fin interacting with the primary vortices from the body as the model is yawed. This particular phenomenon will be the focus of future experimental testing.

4.3 Full Configuration with Control Surfaces Deflected

A series of tests were conducted to investigate the effectiveness of the control surfaces. This involved configuring the model in its fully-appended state, with transition strip-on, and testing at a free-stream velocity of 60 m/s. The model was pitched, at zero β, and then yawed, at zero α, with the control surfaces deflected to induce both positive and negative pitch and yaw motions. Four control surfaces with discrete deflection angles of 3° were used for these tests.

4.3.1 Effect of Aft Control Surfaces on Pitch

Pitch control was achieved by deflecting all four control surfaces in unison to induce either a nose-up or a nose-down response. For nose-up pitch attitude, all control surfaces were deflected 3° trailing-edge up, and conversely, nose-down pitch attitude was achieved by deflecting all control surfaces 3° trailing-edge down. Figure 7 presents schematic diagrams to indicate the control surface deflections for pitch control, based on the convention defined in reference 5.

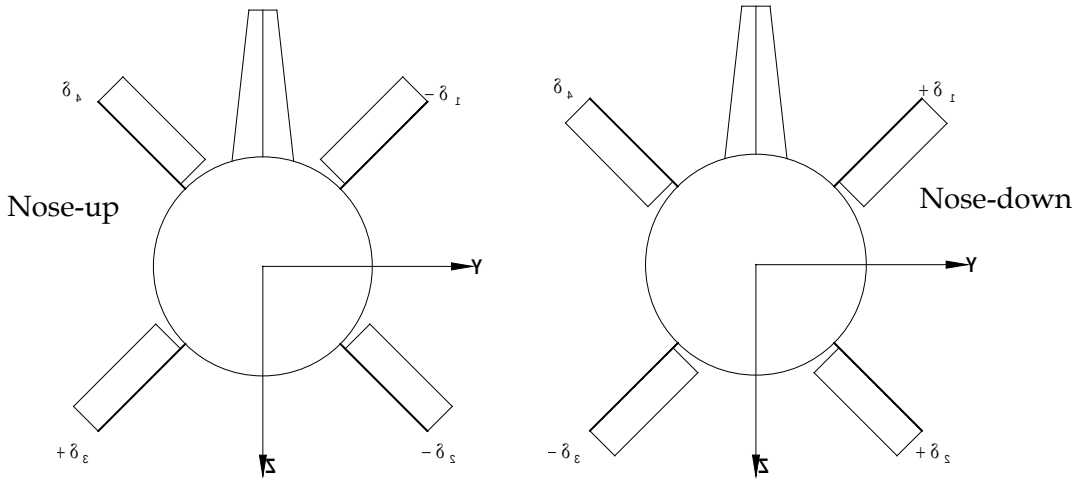

Figure 7 – Combination of control surface deflection angles used for pitch control.

Figure E 1 shows results for each of the force and moment coefficients when the model is pitched through a range of α at zero β, where the control surfaces were fixed in their neutral position (i.e. zero deflection); and for the control surfaces deflected to achieve nose-up and nose-down pitch.

Generally, the trends in the data are consistent over the range of conditions tested. Both C_M and C_Z data show the effects of deflecting the control surfaces, with predictable changes in the magnitudes of these coefficients. Furthermore, deflecting the control surfaces to initiate pitch motion (a pitch moment), does not significantly influence the C_K, C_Y, and C_N coefficients.

Figure E 2 shows results for each of the force and moment coefficients when the model is yawed through a range of β at zero α for the controls fixed in their neutral position (i.e. zero deflection); and for the controls deflected to achieve either nose-up or nose-down pitch attitude.

The C_K, C_Y, and C_N coefficients are not influenced by the pitch deflection settings of the control surfaces over the range of drift angle tested. However, the results for the surge-force coefficient (C_X) indicate significant variations, particularly at moderate drift angles (i.e. β =15°). These trends in the data represent discrete changes in the flow-field, and are most likely due to the interaction of the vortex structures emanating from the fin and the hull-casing.

4.3.2 Effect of Aft Control Surfaces on Yaw

Yaw control was achieved by deflecting all four control surfaces (i.e. by 3°) in combination to induce either a yaw-starboard or yaw-port. Figure 8 presents the control surface deflections for yaw control based on the convention for control surfaces defined in reference 7.

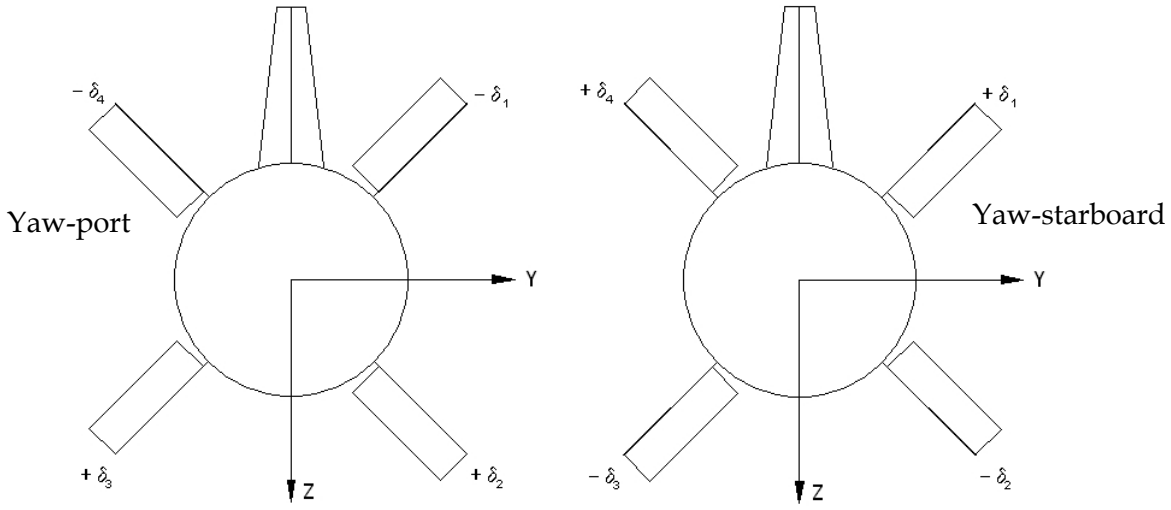

Figure 8 – Combination of control surface deflection angles used for yaw control.

Figure F 1 shows results for each of the force and moment coefficients when the model is pitched through a range of α at zero β and includes data for the control surface fixed in their neutral position, as well as for control surfaces deflected to induce yaw-starboard and yaw-port.

The effects due to the deflected control surfaces are evident in the roll moment (C_K) plot, and to a lesser degree in the yaw-moment (C_N) data. The plot of sway coefficient (C_Y) indicates minor changes due to the deflected control surfaces, while the C_X, C_Z and C_M coefficients show no significant effects. Overall, the control fins have produced relatively minor yaw control increments, a result that is consistent with the small magnitude of control surface deflections tested, and given that the control fins are located on the aft-body, operating predominantly in a wake region.

Figure F 2 shows results for each of the force and moment coefficients when the model is yawed through a range of β at zero α, and similarly includes data for the control surfaces fixed in their neutral position, as well as for control surfaces deflected to induce yaw-starboard and yaw-port. With the exception of the yaw moment data, the results show that there are no significant effects in the coefficients when the control surfaces are deflected. The increments in C_N produced by the control deflections are also relatively minor due to the dominance of the fin at these drift angles.

4.4 Assessment of Data Quality

Guidelines are provided in [6] for estimating the uncertainties in the instrumentation and data acquisition systems used during the tests. The bias limits shown in Table 3 were estimated from the standard errors for the calibration of the measuring instrument, while the precision limits were obtained from the standard deviations of 50 data samples at each measuring point. When there is no sampling statistics (e.g. strain gauge balance calibration where the sampling information was not provided by the supplier) the precision limit is not calculated. The uncertainties were estimated with a 95 percent confidence level (i.e. 2σ) using the methodology outlined in [6].

Table 3 - Estimated uncertainties for the instrumentation and the low speed wind tunnel data acquisition system

Description	Bias Limit	Precision Limit	Calibration Uncertainty	Calibration Range	Measuring Device
Balance					DSTO-BAL-04 six-component strain gauge balance
F_X (N)	± 0.310	---	± 0.310	± 60	
F_Y (N)	± 0.600	---	± 0.600	± 500	
F_Z (N)	± 1.260	---	± 1.260	± 500	
K (Nm)	± 0.128	---	± 0.128	± 5	
M (Nm)	± 0.073	---	± 0.073	± 25	
N (Nm)	± 0.092	---	± 0.092	± 25	
Inclinometer					Jewel LCF-3000 tri-axial inclinometer for pitch. Yaw angle measured from turntable encoder
Pitch (°)	± 0.029	± 0.023	± 0.04	± 45	
Yaw (°)	± 0.100	---	± 0.10	± 180	
Dynamic Pressure (kPa)	± 0.0019	± 0.0039	± 0.0043	± 20	Digiquartz differential pressure transducer, calibrated using a dead weight pressure calibrator
Total Pressure (kPa)	± 0.0046	± 0.0050	± 0.0068	96 – 104	Digiquartz absolute pressure transducer, calibrated using a standard pressure balance

Furthermore, uncertainties for selected parameters are also stated, and were estimated using the methodology outlined in [6]. These estimates are shown in Table 4 and were based on the statistical data during a typical run.

Table 4 - Estimated uncertainties for selected parameters during a typical run

Description	Bias Limit	Precision Limit	Uncertainty	Nominal Value
Geometry				
Reference Length, l (m)	0.0005	---	0.0005	1.35
Reference Area, S (m^2)	2.5×10^{-7}	---	2.5×10^{-7}	1.8225
Test Conditions				
q (kPa)	---	0.0050	0.0024	2.25
U (ms^{-1})	---	0.0460	0.0100	60.00
P_T (kPa)	---	0.0040	0.0050	104.65
Up-flow (°)	---	0.0500	0.0500	1.80
Cross-flow (°)	---	0.0500	0.0500	0.24
Model Attitude				
Angle-of-attack, α (°)	0.04	0.006	0.04	15.0
Angle of drift, β (°)	0.10	0.02	0.10	0.0
Forces & Moments				
F_X (N)	0.31	0.240	0.393	-75.83
F_Y (N)	0.60	0.120	0.612	-18.63
F_Z (N)	1.26	0.140	1.268	-394.55
K (Nm)	0.13	0.006	0.130	0.452
M (Nm)	0.07	0.600	0.604	23.739
N (Nm)	0.09	0.100	0.135	0.365
Body-axes Coefficients				
C_X	0.00008	0.00006	0.00010	-0.0185
C_Y	0.00015	0.00003	0.00015	-0.0045
C_Z	0.00032	0.00004	0.00032	-0.0962
C_K	0.00002	0.000001	0.00002	0.0001
C_M	0.00001	0.00011	0.00011	0.0043
C_N	0.00002	0.00002	0.00003	0.0001

5. Conclusion

DSTO researchers have successfully completed a series of low-speed wind tunnel tests on a generic submarine model. These tests were used to gather gross steady-state force and moment data with the model in various configurations, namely an incremental build-up to a full-configuration, that is, with a hull-casing, fin and control surfaces attached, and with the control surfaces deflected.

This report documents the experimental equipment used during the wind tunnel tests, including descriptions of the model, the test facility, and the instrumentation used to gather the data. Definitions of the axes systems and reference coordinates were also reported, along with the data reduction methods, the corrections applied to the results, the test conditions, and the test schedule. A sample of the data gathered was presented, and these results were briefly discussed. Overall the trends in the data were both predictable and repeatable. Furthermore, there was good consistency in the results when compared with information gathered during previous wind tunnel testing of the model in the same configurations.

The data from these tests adds to a substantial database of information already compiled for this generic submarine shape, and provides a valuable source of comparative data for computational analysis of this same geometry. In addition, there were also a number of practical lessons learned, including the effects of model mounting, and this information will be used to better inform future test programs.

6. Acknowledgements

The authors would like to thank John Clayton, Paul Jacquemin, Kevin Desmond, Alberto Gonzalez, Peter O'Connor, Chris Rider and also QinetiQ contractors, Paul Vella and Michael Vogl, for their assistance in preparing the model and conducting the wind tunnel tests.

7. References

[1] Quick, H., Widjaja, R., Anderson, B., Woodyatt, B., Snowden, A.D., Lam, S., *Phase I Experimental Testing of a Generic Submarine Model in the DSTO Low Speed Wind Tunnel*, DSTO Technical Note, DSTO-TN-1101, July 2012.

[2] Joubert P. N., *Some Aspects of Submarine Design Part 1 – Hydrodynamics*, Defence Science and Technology Organisation Technical Report DSTO-TR-1622, 2004.

[3] Barlow, J. B., Rae, W. H. and Pope, A., *Low-Speed Wind Tunnel Testing*, John Wiley & Sons, 1999.

[4] Braslow, A. L., and Knox, E. C., *Simplified Method for Determination of Critical Height of Distributed Roughness Particles for Boundary Layer Transition at Mach Numbers from 0 to 5*, NACA TN 4363, 1958.

[5] American Institute of Aeronautics and Astronautics (AIAA), *Recommended Practice for Atmospheric and Space Flight Vehicle Coordinate Systems*, AIAA R-004-1992.

[6] American Institute of Aeronautics and Astronautics (AIAA), *Standard – Assessment of Experimental Uncertainty with Application to Wind Tunnel Testing*, AIAA S-071A-1999.

Appendix A Technical Specifications

Table A1 – Specification for DSTO low-speed wind tunnel.

Date Built	Tunnel was completed in late 1941, and entered service in early 1942
Type	Conventional closed-circuit, single-return, continuous flow, low speed wind tunnel
Test Section	Two interchangeable (removable) irregular octagonal 'parallel sided' test sections, 2.74 m wide by 2.13 m high. • Total test section length is 5.71 m, measured forward of pressure equalisation slot. • Parallel test section length upstream of the centre of the mechanical balance, which also corresponds to the centre of the turntable (and typically the model pitch axis), is 4.19 m. • Removable viewing windows in the sides of each test section
Operating Pressure	Atmospheric
Velocity	Nominally 100 m/s when the test section is empty
Reynolds no.	Approximately 1.6×10^6, based on a length scale of $0.1\ A^{1/2}$, where A is the test section cross sectional area of 5.28 m^2 and the airspeed is 100 m/s.
Main Drive System	660 kW (900 hp) electric motor driving a 3.96 m diameter eight bladed fan, with a maximum rotational speed 750 RPM, manually controlled.
Cooling	40 °C (105 °F) is the maximum allowable operating temperature. A chilled water heat exchanger is located in the turning vanes in the 1st corner of the circuit after the test section.
Honeycomb	Triangular cells with the dimensions 48 mm by 41 mm by 41 mm, and 127 mm long are located after the 4th corner of the circuit just before the contraction.
Contraction	4:1 contraction ratio
Screens	No flow manipulation screens, wire mesh safety screen in the 1st diffuser downstream of test section.

Table A2 - DSTO LSWT data acquisition system

Data Acquisition System	• Intel Xeon computer running Red Hat Fedora Linux, providing real-time graphical display, data processing, data storage and printer output. • Force and moment data acquisition provided by Vishay Strain Gauge Amplifiers, using a VXI system controller with Ethernet connection to the main computer. • Data acquisition modules to control the facility equipment (pitch-arm and turn-table), and to acquire data from the wind tunnel instrumentation using PC-based modules.

Table A3 - Strain gauge balance (DSTO-BAL-04)

Strain Gauge Balance (DSTO-BAL-04)	A six-component internal strain gauge balance with the load range: **Range** • Axial force (X) ±100N • Side force (Y) ±1000N • Normal force (Z) ±1000N • Roll moment (K) ±12Nm • Pitch moment (M) ±50Nm • Yaw moment (N) ±50Nm
	Standard Errors • Axial force (X) ±0.154% F.S. • Side force (Y) ±0.030% F.S. • Normal force (Z) ±0.063% F.S. • Roll moment (K) ±0.534% F.S. • Pitch moment (M) ±0.073% F.S. • Yaw moment (N) ± 0.092% F.S

Appendix B Test Schedule

Table B1 – Force and moment testing of the generic submarine model

Test No.	Model Configuration									Test Parameters		Notes
	Hull		Casing	Fin	Control Surfaces							
		Trip Strip			Description	Deflection Angles				Vel.	Angle List	
						Port Upper	Port Lower	Stbd Lower	Stbd Upper	(m/s)	Phase 1 (2010) Table: Pitch #1 x Yaw #3 (361pts)	
1	Hull Only	No Trip	Off	Off	Off					30, 40, 60	Pitch #1 (19 pts) Yaw #3 (19 pts)	Check on 2010 Data Set
2	Hull Only	Std	Off	Off	Off					60	Phase 1 Table: (361pts)	Check on 2010 Data Set
3	Hull Only	Std	Off	Off	Off					30, 40, 60	Pitch #1 (19 pts) Yaw #3 (19 pts)	Check on 2010 Data Set
4	Hull Only	Std	Off	Off	Off					60	Pitch #1 (19 pts) {Yaw +/-30; +/-25}	Data checks
5	Hull	Std	Off	Off	4 x stern	0	0	0	0	60	Pitch #1 (19 pts) Yaw #3 (19 pts)	Control Surface Effect
6	Hull	Std	ON	FIN #1	4 x stern	0	0	0	0	60	Phase 1 Table: (361pts)	Full Configuration: Casing, Fin, Control Surfaces
7.1	Hull	Std	ON	FIN #1	Deflected	**. +3**	**. +3**	**-3**	**-3**	60	Pitch #1 (19 pts) Yaw #3 (19 pts)	Pitch-Down case
7.2	Hull	Std	ON	FIN #1	Deflected	**-3**	**-3**	**. +3**	**. +3**	60	Pitch #1 (19 pts) Yaw #3 (19 pts)	Pitch-Up case
7.3	Hull	Std	ON	FIN #1	Deflected	**. +3**	**-3**	**-3**	**. +3**	60	Pitch #1 (19 pts) Yaw #3 (19 pts)	Yaw Right case
7.4	Hull	Std	ON	FIN #1	Deflected	**-3**	**. +3**	**. +3**	**-3**	60	Pitch #1 (19 pts) Yaw #3 (19 pts)	Yaw Left case
7.5	Hull	Std	ON	FIN #1	Deflected	0	0	**-3**	**-3**	60	Pitch #1 (19 pts) Yaw #3 (19 pts)	Roll to Stbd case (2 x Control Surfaces)
7.6	Hull	Std	ON	FIN #1	Deflected	0	0	**. +3**	**. +3**	60	Pitch #1 (19 pts) Yaw #3 (19 pts)	Roll to Port case (2 x Control Surfaces)
7.7	Hull	Std	ON	FIN #1	4 x stern	0	0	0	0	60	Pitch #1 (19 pts) Yaw #3 (19 pts)	Control Surfaces neutral Check Case
8	Hull	Std	ON	FIN #1	Off					60	Pitch #1 (19 pts) Yaw #3 (19 pts)	Fin Effect
9	Hull	Std	ON	Off	4 x stern	0	0	0	0	60	Pitch #1 (19 pts) Yaw #3 (19 pts)	Casing & Control Surfaces Effect
10	Hull	Std	ON	Off	Off					60	Pitch #1 (19 pts) Yaw #3 (19 pts)	Casing Effect
11	Hull Only	Std	Off	Off	Off					60	Pitch #1 (19 pts) Yaw #3 (19 pts)	Repeat Case (Config. 2) Final Run

Phase 1 Angle List
Sub. Model Angles
(As Tested, 2010)

Pitch Angles																			
Set #1	[-15.0	-10.0	-7.0	-5.0	-4.0	-3.0	-2.0	-1.0	-0.5	0.0	0.5	1.0	2.0	3.0	4.0	5.0	7.0	10.0	15.0]

Yaw Angles																			
Set #3	[-30.0	-20.0	-10.0	-5.0	-1.0	-0.5	0.0	0.5	1.0	2.0	3.0	4.0	5.0	7.0	10.0	15.0	20.0	25.0	30.0]

Appendix C Reference Runs

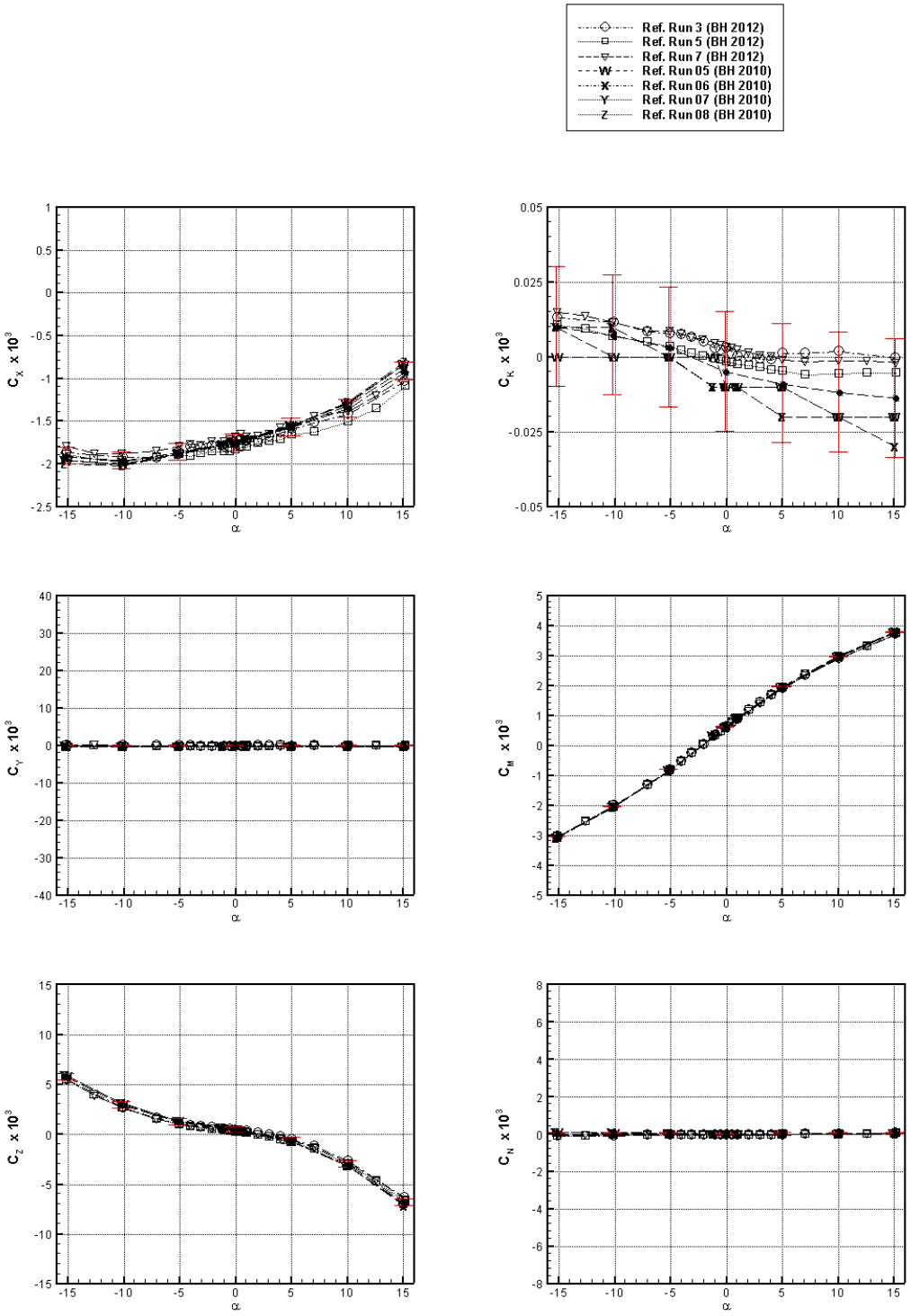

Figure C1 – Reference Runs - Force and moments coefficients versus a.

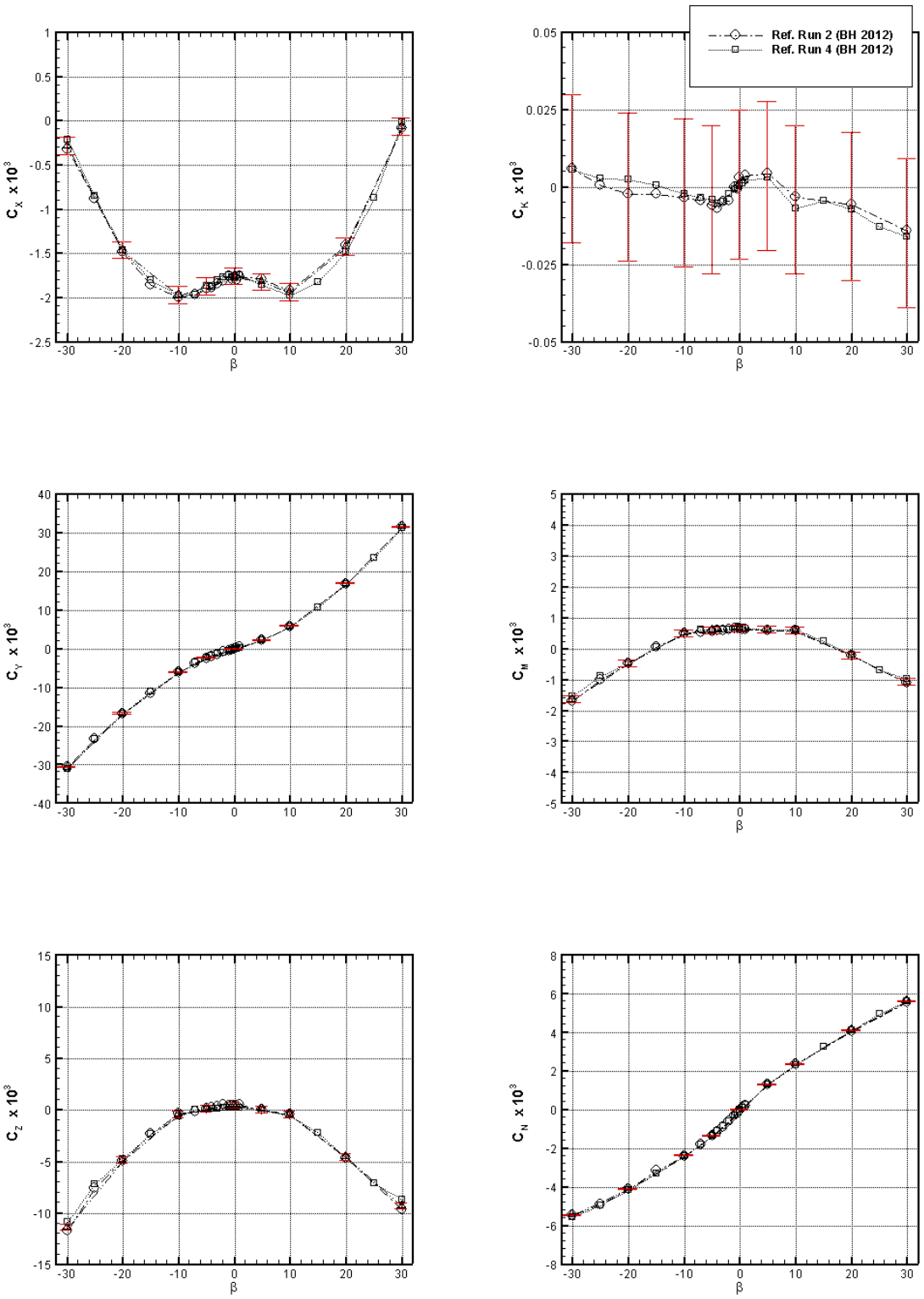

Figure C2 – Reference Runs - Force and moment coefficients versus β.

Appendix D Bare-Hull plus Appendages

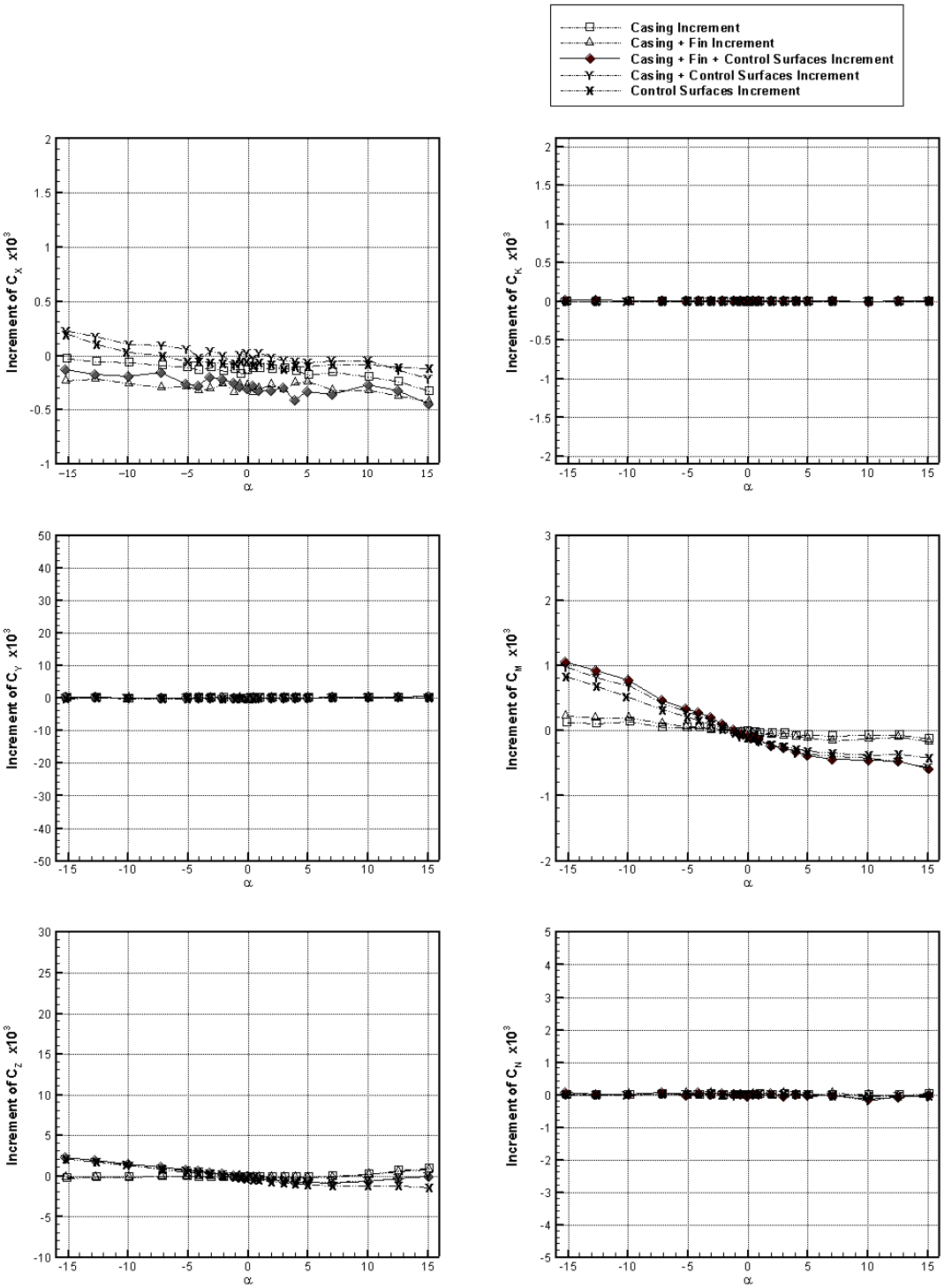

Figure D1 - Incremental body-axes force and moment coefficients versus a for the model fitted with various appendages.

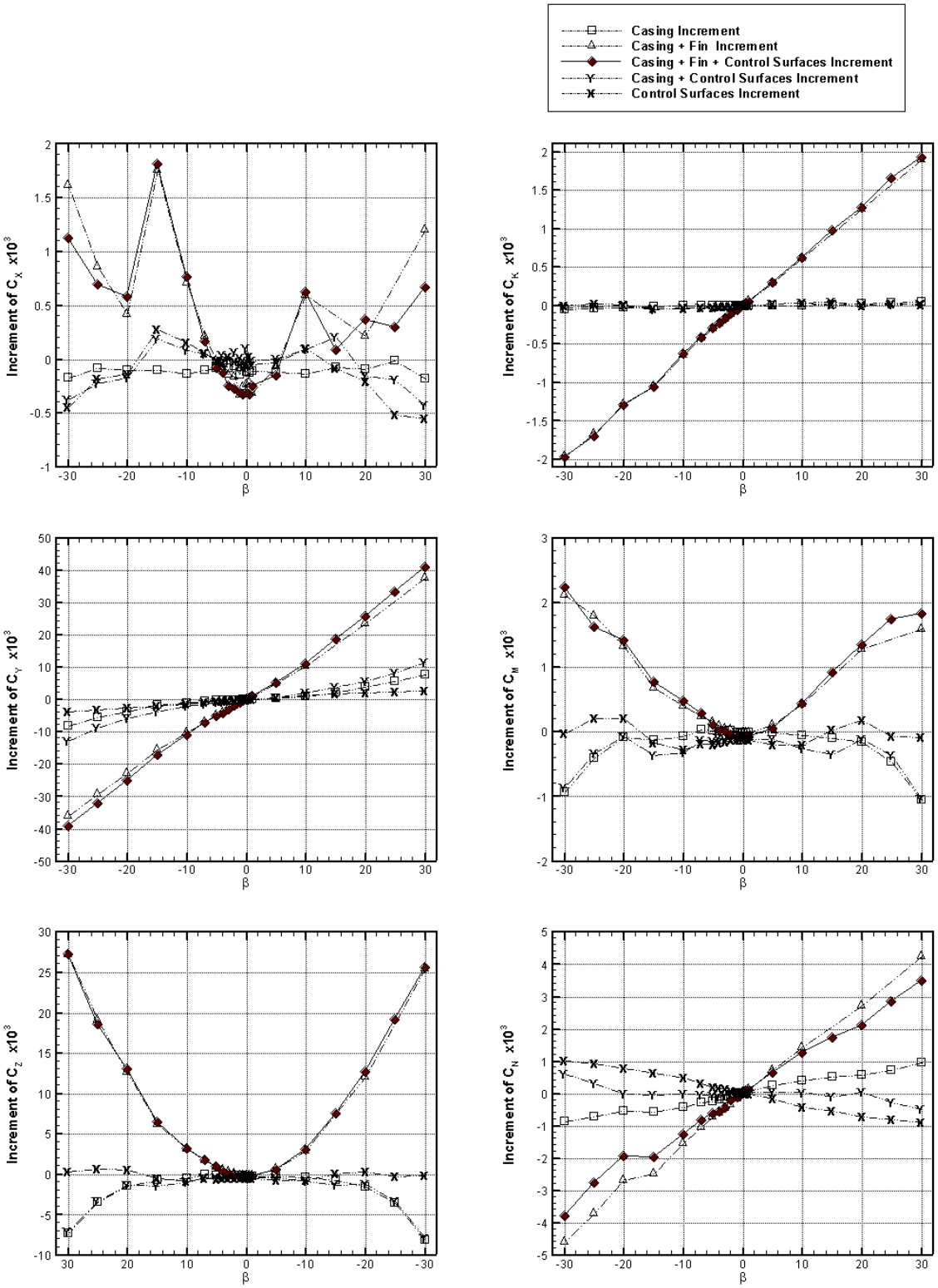

Figure D2 - Incremental body-axes force and moment coefficients versus β for the model fitted with various appendages.

Appendix E Effect of Aft Control Surfaces on Pitch

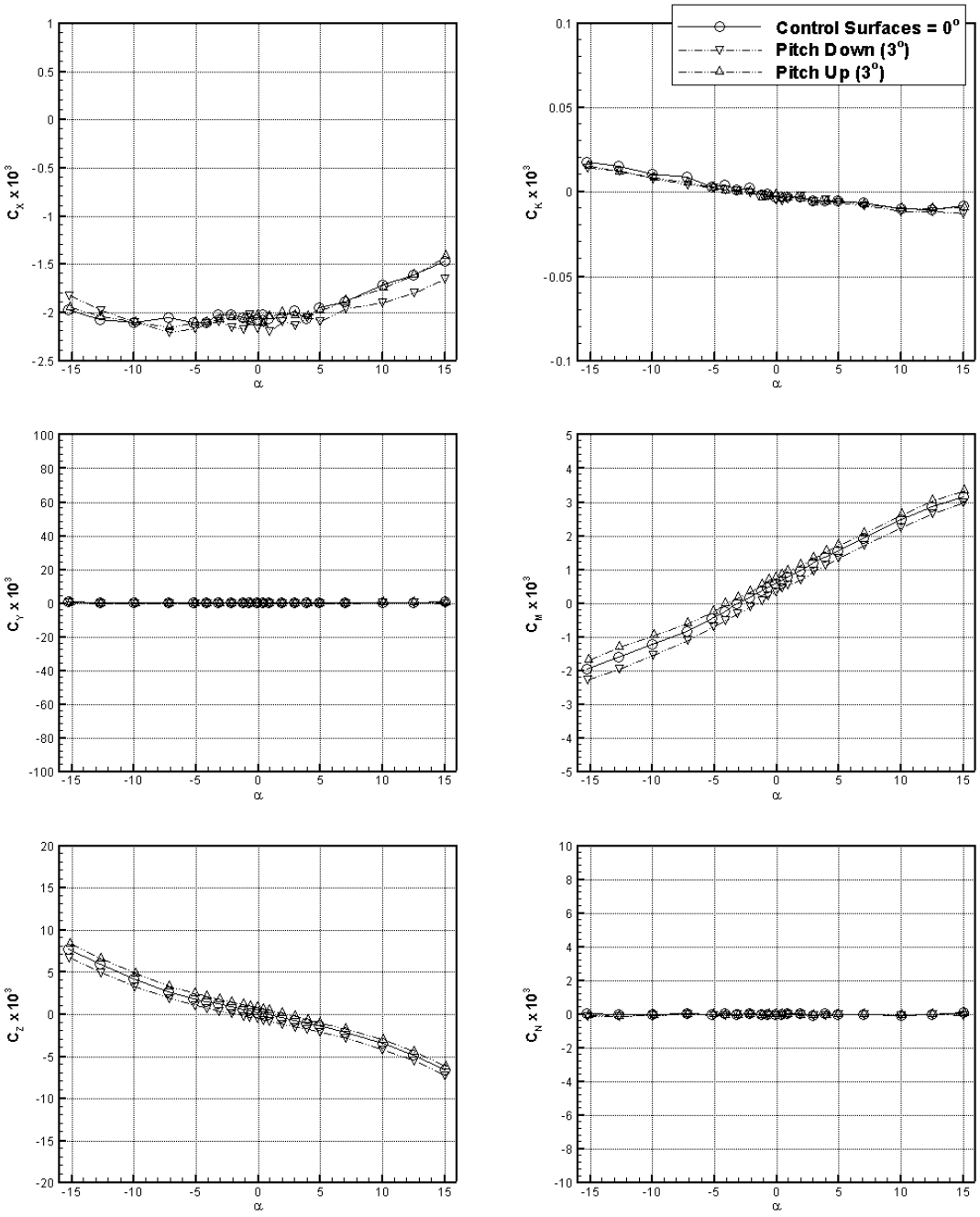

Figure E1 - Body-axes force and moment coefficients versus a with control surfaces deflected for pitch.

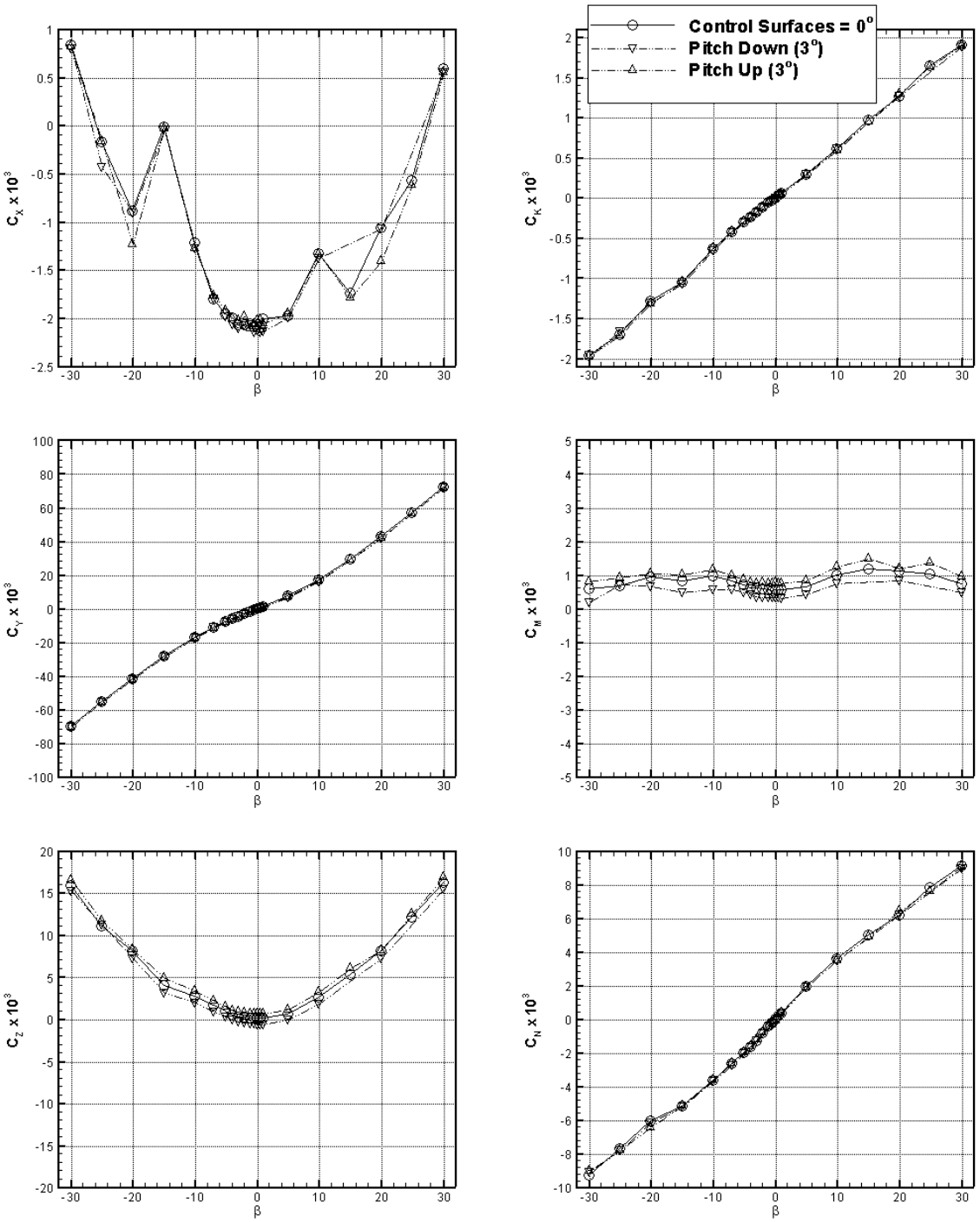

Figure E2 - Body-axes force and moment coefficients versus β with control surfaces deflected for pitch.

Appendix F Effect of Aft Control Surfaces on Yaw

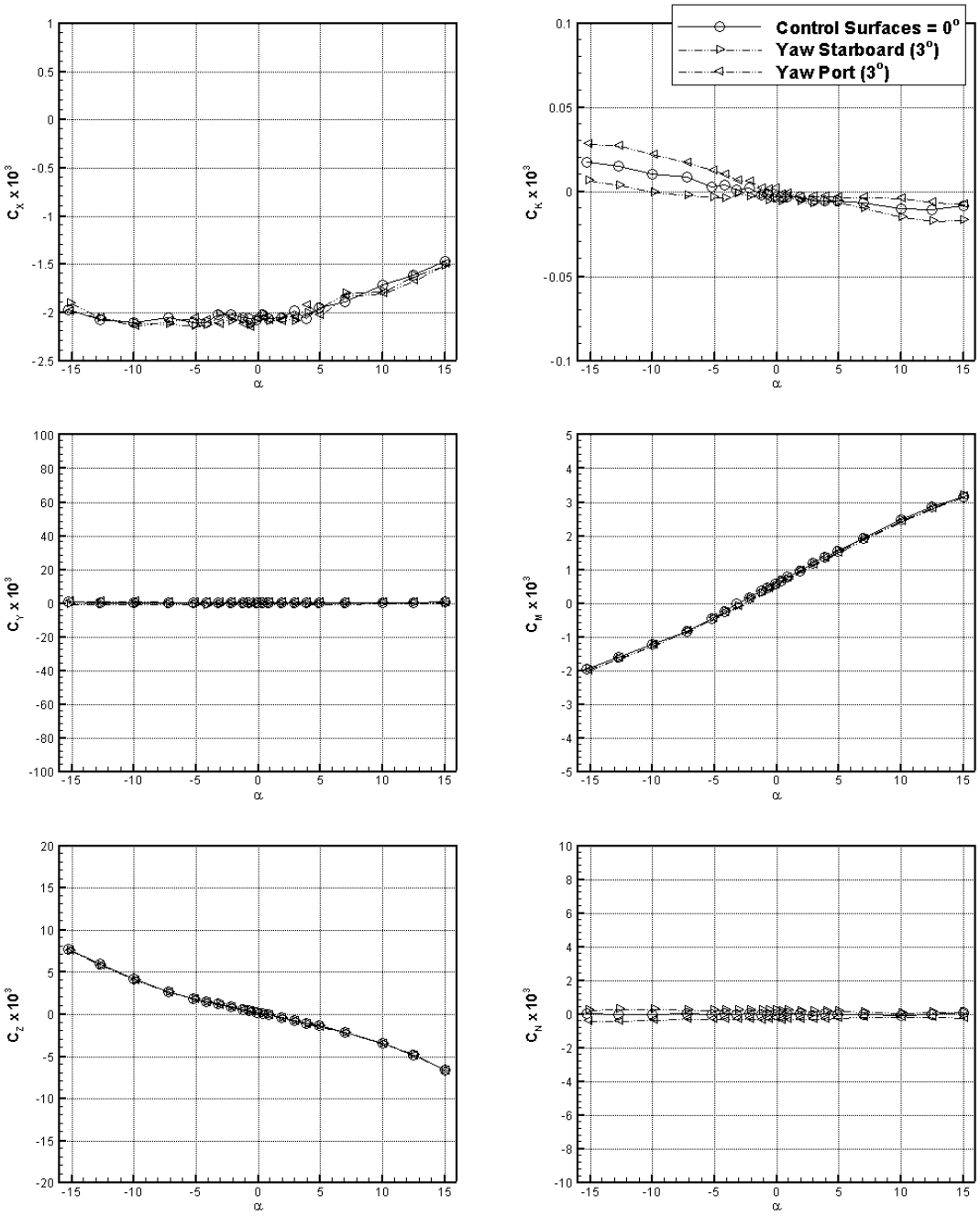

Figure F1 - Body-axes force and moment coefficients versus a with control surfaces deflected for yaw.

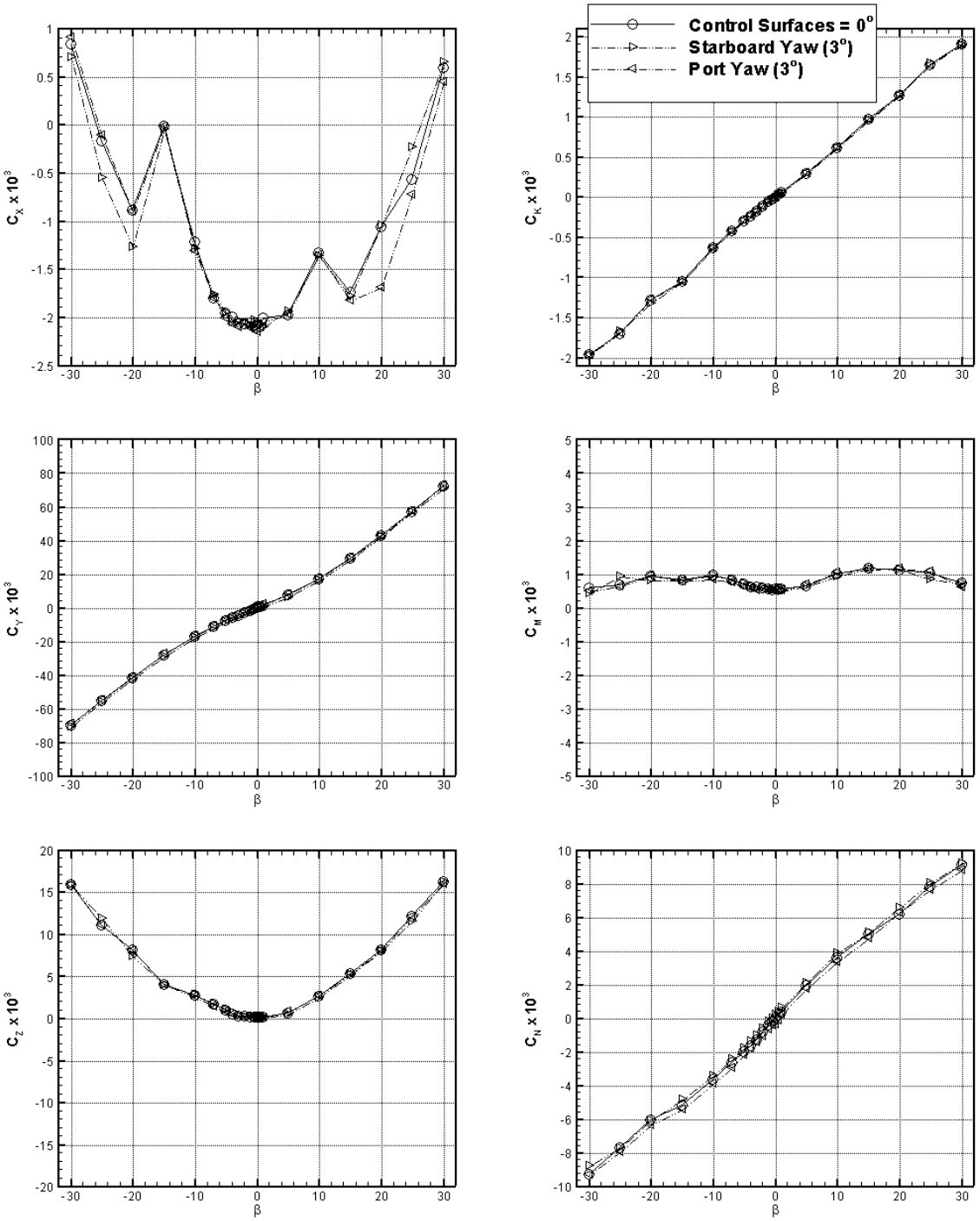

Figure F2 - Body-axes force and moment coefficients versus β with control surfaces deflected for yaw.

DEFENCE SCIENCE AND TECHNOLOGY ORGANISATION
DOCUMENT CONTROL DATA

1. DLM/CAVEAT (OF DOCUMENT)

2. TITLE

Phase II Experimental Testing of a Generic Submarine Model in the DSTO Low Speed Wind Tunnel

3. SECURITY CLASSIFICATION (FOR UNCLASSIFIED REPORTS THAT ARE LIMITED RELEASE USE (L) NEXT TO DOCUMENT CLASSIFICATION)

Document	(U)
Title	(U)
Abstract	(U)

4. AUTHOR(S)

Howard Quick and Bruce Woodyatt

5. CORPORATE AUTHOR

DSTO Defence Science and Technology Organisation
506 Lorimer St
Fishermans Bend Victoria 3207 Australia

6a. DSTO NUMBER	6b. AR NUMBER	6c. TYPE OF REPORT	7. DOCUMENT DATE
DSTO-TN-1274	AR-015-873	Technical Note	March 2014

8. FILE NUMBER	9. TASK NUMBER	10. TASK SPONSOR	11. NO. OF PAGES	12. NO. OF REFERENCES
	07/299	DSTO	29	6

13. DSTO Publications Repository

http://dspace.dsto.defence.gov.au/dspace/

14. RELEASE AUTHORITY

Chief, Aerospace Division

15. SECONDARY RELEASE STATEMENT OF THIS DOCUMENT

Approved for public release

OVERSEAS ENQUIRIES OUTSIDE STATED LIMITATIONS SHOULD BE REFERRED THROUGH DOCUMENT EXCHANGE, PO BOX 1500, EDINBURGH, SA 5111

16. DELIBERATE ANNOUNCEMENT

No Limitations

17. CITATION IN OTHER DOCUMENTS Yes

18. DSTO RESEARCH LIBRARY THESAURUS

Submarine hulls; wind tunnel tests; aerodynamic loads

19. ABSTRACT

DSTO has completed the second phase of an experimental test program on a sub-scale model of a generic submarine in its low-speed wind tunnel. These tests were used to gather gross steady-state aerodynamic force and moment data for the model in various configurations, where different appendages including a hull-casing, a fin, and control surfaces were incrementally added to the bare-hull form. The effectiveness of the control surfaces to induce pitch and yaw motions was also investigated.